Electrical Power and Energy Systems 157 (2024) 109869

Contents lists available at ScienceDirect

International Journal of Electrical Power and Energy Systems

journal homepage: www.elsevier.com/locate/ijepes

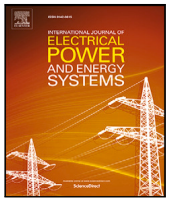

Techno-economic analysis of electrical flexibility in combustion-based district heating systems: A Swiss case study

Roberto Rocca [a,b,*], Lorena Elorza-Uriarte [a], Itziar Zubia [c], Daniele Farrace [d], Riccardo Toffanin [d], David Miguel Rivas-Ascaso [a]

[a] Electrical Systems Department of CIRCE Technology Centre, Av. de Ranillas, 3D, 1°, Zaragoza, 50018, Spain
[b] CIRCE Mixed Research Institute (CIRCE Technology Centre and University of Zaragoza), C. de Mariano Esquillor Gómez, Zaragoza, 50018, Spain
[c] Electrical Engineering Department of the University of the Basque Country UPV/EHU, Plaza Europa 1, Donostia-San Sebastián, 20018, Spain
[d] Azienda Elettrica di Massagno (AEM), Via Lisano 3, Massagno, 6900, Switzerland

ARTICLE INFO

Keywords:
Control
Demand response
District heating
Flexibility
Local flexibility market
Market bid
Modelling
Sector coupling

ABSTRACT

Nowadays, the expected growth of local flexibility markets and demand-response mechanisms is urging researchers and practitioners to obtain flexibility from all possible devices, including those historically considered as "stiff". To this end, this work proposes an alternative control strategy for combustion-based district heating systems allowing the pumping system to operate as a flexible load. The idea is investigated via simulation in the case study of Capriasca (Lugano), within the framework of the EU-H2020-ACCEPT project. Starting from historical on-field measurements of heat consumption, a techno-economic analysis is conducted upon the flexibility obtainable from the pumping system, along with its cost, in two different scenarios: (i) participation in a local flexibility market and (ii) participation in a demand response program. Eventually, further to proving the viability of the proposed idea, the analysis shows that percent flexibility between 25% and 70% of the pumping system rated power can be reached, depending on the heat consumption. The additional economic advantages of flexible DHS operation in low electricity price scenarios are also highlighted.

1. Introduction

In a bid to counteract the irreversible effects of global warming and climate change phenomena, an energy transition is currently ongoing that pursues a fully decarbonised economy by 2050 [1]. This transition demands massive amounts of renewable energy systems to be installed, posing the inherent problem of matching instantaneously energy generation and demand. Additionally, when installed at distribution grid level, excess of renewable generation may cause technical issues such as overvoltage and congestion.

Together with the installation of energy storage systems [2–4], demand-side management currently represents a valuable means to integrate higher shares of renewable generation in distribution grids [5]. In demand-side management, consumers are invited to change their consumption patterns via monetary incentives. This scenario introduces two key concepts, namely flexibility and Demand-Response (DR). Flexibility is referred to as the ability of increasing or decreasing a consumer's electricity demand in response to an external signal [6,7]. In particular, flexibility is becoming an indispensable means to prevent and/or solve distribution grids issues, which is paving the way to the creation of Local Flexibility Markets (LFMs) where customers can sell flexibility to Distribution System Operators (DSOs) [8,9]. Besides, flexible loads can be exploited in DR schemes. In this case, consumers are offered either time-dependent energy tariffs or one-shot monetary incentives, named tokens, to change their foreseen consumption and thus help solving or preventing grids issues [7,10–12].

The expected growth of LFMs and DR schemes is opening new research and engineering pathways aimed at obtaining flexibility from any available device, including those that have been historically considered as "stiff", i.e., non flexible. Electric Vehicles represent one of the most flexible classes of electric loads, as charging operations can be easily shifted in time or modulated in intensity [6,13,14]. Another promising option lies in the Sector Coupling (SC) [15–19]. This last can be defined as the integration of different energy vectors with one another, with the aim of maximising synergies between them. A typical example of SC is provided by the Heating Ventilation and Air Conditioning (HVAC) systems based on Heat Pumps (HPs), where thermal energy demand, naturally more flexible, turns into a shiftable electric demand [20,21].

Another interesting example of SC lies in the residential districts, where several energy vectors are normally involved. In the field of

* Corresponding author at: Electrical Systems Department of CIRCE Technology Centre, Av. de Ranillas, 3D, 1°, Zaragoza, 50018, Spain.
E-mail address: roberto.rocca@ieee.org (R. Rocca).

https://doi.org/10.1016/j.ijepes.2024.109869
Received 4 August 2023; Received in revised form 16 November 2023; Accepted 11 February 2024
Available online 16 February 2024

the so-called multi-energy districts, the most complex yet complete case of district-level SC, with electricity, gas and heating networks being simultaneously optimised is addressed in [22–24], with the main contribution lying in the mathematical formulation of the optimal technical dispatch problem. Additionally, [25,26] address the market aspects of the three-vector problem by proposing a network-secure bidding optimisation accompanied by a model predictive control.

By moving to research works focusing only on district-level electricity and heat coupling, different objectives are pursued in the literature. M. Majidi presents a day-ahead optimisation framework for a smart district, where the main objective is once again the optimal technical dispatch problem [27]. A. A. Bashir [28] and I. Hadachi [29] propose two mixed-integer linear-programming frameworks that exploit the flexibility provided by both Combined Heat and Power Systems (CHPSs) and EV fleets.

By focusing on contributions that take only the heat generation/distribution system into account, a wide agreement is found that electric flexibility can be obtained via two types of energy assets, namely CHPSs and HPs, as it is shown in [30] in the Barry Island practical case study. Y. Cao [31] and J. Tan [32] propose respectively a market-driven optimal operation schedule that takes into account the effects on the electric distribution network, and a strategic investment scheme for a District Heating System (DHS) participating in both electricity and reserve markets. Eventually, if only CHPS is taken into account, an optimal dispatch is presented in [33], where the available flexibility is enhanced through a variable mass flow operation. On the other hand, X. Xu [34], rather than focusing on the optimal dispatch problem, tackles the flexibility quantification.

The above analysis shows that all main sources of district-level flexibility are flexible by nature. In the particular case of CHPSs, flexibility is obtained directly by modulating the ratio between heat and electricity production. As opposed to it, in simple DHSs, all energy from fuel combustion is used to produce hot water, with a relatively small electric consumption provided by the pumping system. For this reason, DHSs have been historically considered as "stiff" electric loads, with research efforts normally focusing on other aspects, such as modelling of heat losses [35,36], exploiting thermal inertia and thermal storage [37–39] or handle failure events [40]. From a more electrical perspective, research works mainly focus on pumping system controls aimed at optimising the electric consumption [41–44].

From all the above, the following observations can be done. Firstly, although in many countries conventional DHSs are more numerous than CHPSs [45], research works on flexibility direct their efforts only towards CHPSs, whereas DHSs remain almost unexplored. In particular, novel solutions to untap flexibility from DHSs, which have been historically considered as electrically "stiff", have not been investigated. Secondly, flexibility quantification has been conducted only for CHPSs and only from a technical perspective, [34], whereas no analyses have been conducted for DHSs. To this end, this work wishes to propose an alternative control strategy for combustion-based DHSs allowing the pumping system to operate as a flexible load. Here, it is necessary to highlight that DHSs are not usually designed for a flexible pumping operation, so that the proposed idea poses the risk of exceeding the rated pressure of pumping and pipes systems. As a countermeasure, an anti-over-pressure droop control is proposed as an additional element of innovation.

To recap, in a bid to fill the bespoke gaps found in the literature, this work wishes to provide a threefold contribution:

1. Propose an alternative control strategy for combustion-based DHSs that untaps the electric flexibility available in the pumping system, which is developed together with a DHSs modelling technique suitable for flexibility evaluation.
2. Provide a techno-economic analysis of DHSs flexible operation when participating in:
   - LFMs.
   - DR schemes.
3. Introduce an anti-over-pressure droop control.

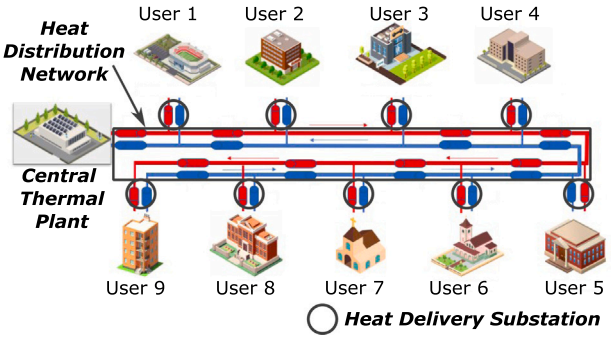

Fig. 1. Simplified example of DHS.

The idea is investigated in the DHS of Capriasca (Lugano), a small, semi-rural village in the Swiss Prealps, demo site of the H2020 ACCEPT project [46]. Here, the viability of the idea is assessed, and a techno-economic analysis is conducted starting from historical on-field measurements of heat consumption of a typical and a heavy winter day.

This paper is structured as follows. Section 2 provides the theoretical background of both DHSs and flexibility. Section 3 presents the proposed "flexible" pumping control strategy, while the DHS modelling is developed in Section 4. Finally, the Capriasca case study is presented in Section 5, whose results are shown and discussed in Section 6.

2. District heating background and flexibility definition

2.1. Main DHS components

A DHS is a centralised system that generates hot water in one or more thermal plants and delivers it to several end-users through a piping network. A simplified example is shown in Fig. 1, where its main components can be seen:

- One or more central thermal plants, where cold water returning from the users is heated up, either in a boiler (gas-fired, wood-fired, etc.) or in a HP. The heat-producing unit, in turn, can be either connected directly to the end-users or through a storage tank.
- A heat distribution network, where hot water is taken from the thermal plant, mixed with some cold water returning from the consumers and eventually pressurised to be sent to the end-users. Usually, this circuit is referred to as "primary" and counts with one or more pumping stations.
- Heat delivery substations, where hot water is delivered to the end-users.
- Users internal hot-water distribution systems, which are usually referred to as "secondary".

2.2. Traditional "stiff" control strategy

In a combution-based system, a control loop regulates the combustion process at thermal-plant level. Besides, at primary-circuit level, two control loops operate in a coordinate way to regulate the hot water distribution. The two loops are shown in Fig. 2. Firstly, the pump controller regulates the hot water flow within the piping system. For this task, several control techniques are available [44]. This work considers the relatively common option of setting a specified differential pressure dP_{ref} to the remotest user. Secondly, hot water is delivered to the users at a lower temperature compared to that leaving the thermal station.

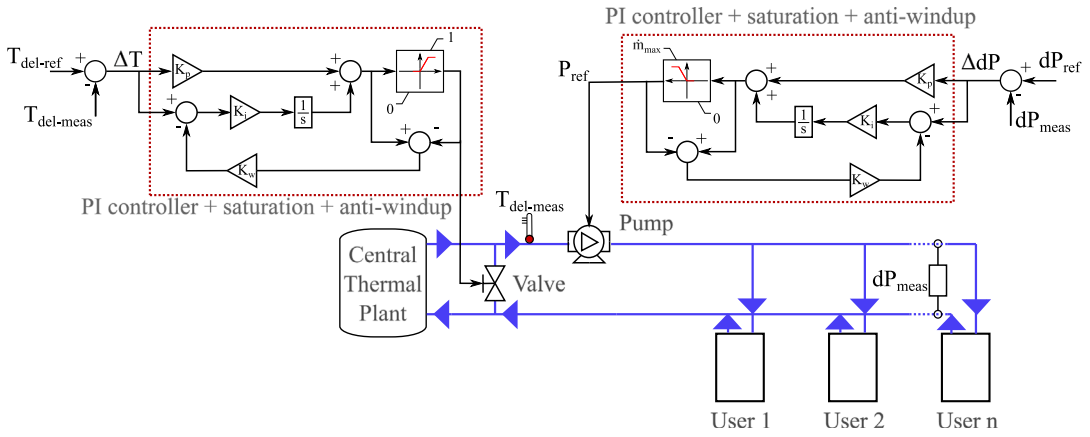

Fig. 2. Distribution control loops: pump and mixing valve.

This task is accomplished by a mixing valve, which mixes cold water returning from the users to the hot water stored in the tank. To this end, the valve opening is modulated via a PI controller based on the difference between the set-point delivery temperature $T_{del-ref}$ and its measured value $T_{del-meas}$. This third control loop has the fundamental role of decoupling hot-water production and distribution, providing so a considerably faster response to heat demand variations, compensating so for the high inertia of the thermal station.

In the way DHSs are normally operated, $T_{del-ref}$ is kept constant. Then, in case an end-user rises its heat demand, its internal control system acts to receive a higher hot-water mass flow rate from the primary circuit. Subsequently, a higher primary mass flow rate increases the pressure drops in the circuit, causing the pump PI to increase the pressure and hence the electricity consumption. At the same time, the variation in absorbed heat causes hot water to return at a lower temperature, so that the mixing valve also kicks in to take hot-water delivery temperature back to $T_{del-ref}$.

2.3. Flexibility markets and demand response general aspects

2.3.1. Flexibility

As already mentioned, flexibility ϕ is referred to as the ability of increasing or decreasing the electricity demand in response to an external signal. In particular, an increased electricity demand $P_{el}|_{up}$ results in the so-called downwards flexibility ϕ_{do}, whereas a decreased one $P_{el}|_{do}$ in upwards flexibility ϕ_{up}. Both ϕ_{do} and ϕ_{up} need to be evaluated with respected to the baseline consumption $P_{el}|_{baseline}$, so that:

$$\phi_{do/up}(t) = P_{el}(t)|_{up/do} - P_{el}(t)|_{baseline}. \quad (1)$$

It is now observed that the variation in electricity consumption is usually related to a cost. In the case of fully electrical loads, such as EVs, HPs, etc., only electricity price needs to be considered. Conversely, a DHS represents a typical example of SC, where flexibility is obtained by shifting energy demand from the electrical to the thermal vector and vice versa. As a result, to assess the flexibility cost, the variations in both electricity and fuel costs, Δc_{el} and Δc_{fuel} respectively, need to be considered:

$$\Delta c_{el} = \int_T \pi_{el}(t)(P_{el}(t)|_{up/do} - P_{el}(t)|_{baseline})dt, \quad (2)$$

$$\Delta c_{fuel} = \int_T \pi_{fuel}(t)(Q_{del}(t)|_{up/do} - Q_{del}(t)|_{baseline})dt, \quad (3)$$

being T a generic time period, Q_{del} the thermal power delivered by the primary circuit and π_{el} and π_{fuel} the electricity and fuel prices.

2.3.2. Local flexibility markets

One of the ways for DSOs to cope with over-voltage and congestion issues is to activate flexibility mechanisms and thus remunerate users that agree to change their foreseen demand (baseline). In this context, LFMs provide a marketplace where flexibility is traded between DSOs and consumers, either directly or with an intermediary aggregator [9,47]. Then, an auction process is opened and all users belonging to the distribution grid zone where flexibility is needed are free to bid, taking into account that both reserve and activation are remunerated [48].

In case a DHS operator decides to participate in a LFM, bidding needs to ensure an economic remuneration. To this end, a Minimum Market Bid (MMB) needs to be evaluated in accordance with Δc_{el} and Δc_{fuel}. By reminding that in a SC system energy is shifted from one vector to another, in a DHS the MMB is given by the sum of the variations in fuel and electricity costs, bearing in mind that if the former is positive the latter is negative and vice versa:

$$MMB = \Delta c_{fuel} + \Delta c_{el}. \quad (4)$$

2.3.3. Demand response mechanisms

An alternative way for handling over-voltage and congestion issues in distribution networks is to directly offer customers economic incentives for changing their foreseen demand. In simple words, DSOs constantly forecast the future status of the distribution grid through a series of relevant indicators, such as bus voltages, cables or transformers load level, etc. Then, should one or more indicator exceed a warning or dangerous value, an intervention request is forwarded to retailers and/or aggregators offering them an economic compensation. Further to this request, retailers and/or aggregators provide customers with either an updated time varying tariff (indirect DR), or one-shot payments named tokens (direct DR) [11,12]. By comparing the two approaches, one may notice that modelling a tariff-based DR scenario would require a considerable amount of information, leading to a highly complex analysis that would be out of the scope of this work. Therefore, only the token-based schemes are considered from now on.

At this point, similarly to the LFM case, a DHS operator needs to decide whether to accept a DR incentive or not. In economic terms, an analogous process to the MMB needs to be followed to quantify the Minimum Acceptable Token (MAT), whose definition is given later in Section 5.3.

3. Proposed "flexible" control strategy

Following from the DHS description provided in the previous section, the proposed "flexible" control strategy is now presented. From a more general perspective, the operation of a DHS can be described by expressing the thermal energy balance in a generic time instant t, which can be expressed as in (5), where:

Q_{boil}: is the thermal power produced by the boiler.
Q_{tank}: is the thermal power delivered/absorbed by the tank.
Q_{del}: is the thermal power delivered by the primary circuit.
Q_{dem}: is the thermal power demanded by all users.
Q_{loss}: is the thermal power loss between pipes and soil.
$Q_{us(i)}$: is the thermal power absorbed by the ith user.
$\dot{m}_{pr}$: is the primary circuit hot-water mass flow rate.
c_p: is the hot-water specific heat.
T_{del}: is the hot-water delivery temperature.
T_{ret}: is the hot-water return temperature.
$\dot{m}^{pr}_{us(i)}$: is the ith user hot-water mass flow rate at the primary side.

$$\begin{cases} Q_{boil} + Q_{tank} = Q_{del} = Q_{dem} + Q_{loss}, \\ Q_{dem} = \sum_{i=1}^{n} Q_{us(i)} \\ Q_{del} = \dot{m}_{pr} c_p (T_{del} - T_{ret}), \\ \dot{m}_{pr} = \sum_{i=1}^{n} \dot{m}^{pr}_{us(i)}, \end{cases} \tag{5}$$

Here, it is noted that Q_{del} depends on T_{ret}, which is normally left uncontrolled and depends on Q_{loss} and on whether users are connected through a heat exchanger or not. On the other hand, these relationships are not expressible in a simple closed-form analytical form and hence have been omitted in (5).

Based on (5), thermal power delivery Q_{del} possesses two degrees of freedom, namely $\dot{m}_{pr}$ and T_{del}, provided that T_{ret} is normally left uncontrolled. As opposed to the traditional "stiff" control, where only $\dot{m}_{pr}$ is controlled, this work proposes the novel idea of modifying the reference of T_{del} in response to a flexibility signal, allowing so the pumping system to operate as a flexible electric load . The idea is relatively simple. For a given Q_{dem}, if a lower electricity consumption is desired, hot water set-point may be raised, so that the corresponding mass flow rate decreases along with the electricity consumption. In the other way around, if a higher electric demand is desired, hot water set-point may be lowered to increase the pumping consumption.

The viability of the idea, along with a techno-economic flexibility analysis are investigated in the case study of Capriasca (Lugano), Switzerland, whose modelling is described in the following section.

4. Flexibility-oriented DHSs modelling and anti-over-pressure droop

As mentioned above, in order to prove the proposed idea in a practical case study, this work considers the DHS of Capriasca (Lugano), Switzerland, one of the demo sites of the H2020 project ACCEPT [46]. The network extends for approximately one kilometre and serves nine users, including a sports centre, schools, a church, residential apartments, etc. [49]. A schematic outlook of the network is shown in Fig. 1. This section describes the modelling of all DHS components in the Open Modelica software [50]. In particular, the modelling technique is described, which has been specifically developed for a flexibility techno-economic analysis. Bearing that in mind, the following simplifying hypotheses are introduced:

1. All users are connected in parallel with the primary circuit.
2. All users are connected with a temperature-controlled heat exchanger, in such a way that hot water leaves the exchanger secondary side at a fixed yet constant temperature.
3. Heat exchangers possess a negligible thermal inertia.
4. The boilers and tank system operation is semi-ideal, as explained in the following.
5. Thermal stratification within the tank is neglected.
6. Mixing valve is replaced by an equivalent pump, as also explained in the following.

Table 1
Boilers rated powers and average combustion efficiencies [51,52].

	Wood-fired	Oil-fired
Rated power [kW]	550	500
Average combustion efficiency [%]	86	92

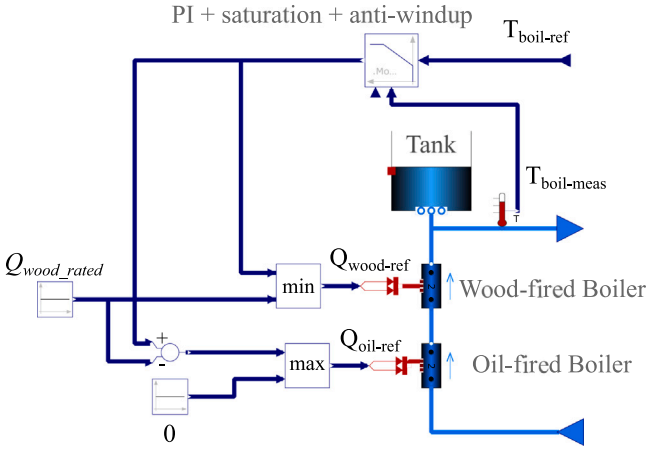

Fig. 3. Boilers model in Open Modelica.

Eventually, it is observed that some of the above hypothesis have been made due to the confidentiality of some information, e.g. connection with the primary circuit or presence of an exchanger. Nonetheless, these simplifications make the DHS model more general, allowing so for an easier generalisation of the results to other DHSs.

4.1. Boiler and tank system

As already said above, the DHS at hand is based on a main wood-fired boiler assisted by an oil-fired one. In the real system, cold water is extracted from the bottom of the tank, at almost the same temperature as the returning water T_{ret}, and circulated through the boilers. As it is common occurrence, the wood-fired one operates in an intermittent way, as it is switched on and off periodically in such a way as to keep combustion efficiency at its highest, while keeping the temperature at the top of the tank within its permitted range.

Following from the hypothesis of a semi-ideal operation, some simplifications are introduced. The boiler and tank system model used in this work is illustrated in Fig. 3. As it can be seen, returning water from the users circulates directly through the boilers. These last are modelled as heat-receiving pipes where an instantaneous combustion takes place, so that produced heat is equal to the required value, $Q_{wood-ref}$ and $Q_{oil-ref}$ respectively. $Q_{wood-ref}$ and $Q_{oil-ref}$ are evaluated via PI controller, equipped with saturation and anti-windup, along with two min/max blocks devoted to the activation of the oil-fired unit when the overall demand exceeds $Q_{wood-rated}$. Combustion efficiencies are assumed to be constants, whose values are reported in Table 1 [51,52].

With regards to the simplification above, by observing (5), it is noted that the limitation of the control system described above lies in the fact that individual contributions Q_{boil} and Q_{tank} cannot be represent accurately. On the other hand, it can also be seen that this simplification ensures the estimation of their sum and hence that of the thermal balance on the right-hand side of (5), which is acceptable for techno-economic analysis purposes. In any case, future efforts are needed to include more accurate boilers models.

4.2. Delivery pump

Fig. 4 illustrates the modelling of the hot-water delivery system, including the delivery pump and the mixing pump. The former is

Table 2
Pumps and electric motor efficiencies.

	Pump	Electric motor
Average efficiency [%]	80	93.75

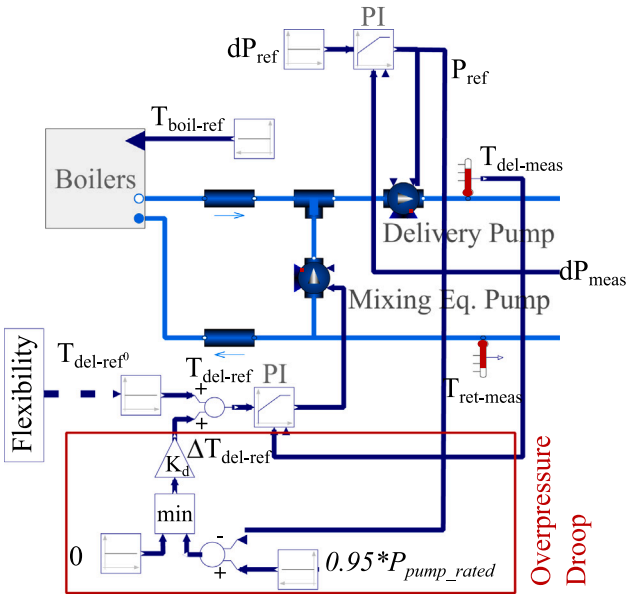

Fig. 4. Hot-water delivery system in Open Modelica.

modelled as a pressure-controlled pump, operating under the action of a PI controller. This last is equipped with saturation and anti-windup and actuates to ensure a 0.5 bar differential pressure to the remotest user. Besides, the limiter is set exactly to the pump rated pressure $P_{pump-rated}$, that is, 7.5 bar. However, it is noticed that operation at $P_{pump-rated}$ is permitted only in temporary conditions, as an anti-over-pressure droop is included that is presented in the next subsection. Pumps electric consumption is expressed through (6), where:

P_{del}: is the water delivery pressure.
P_{ret}: is the water return pressure.
η_{pump}: is the pump mechanical efficiency.
η_{em}: is the pump electric motor efficiency.

Efficiencies are reported in Table 2.

$$P_{el} = \frac{\dot{m}_{pr}(P_{del} - P_{ret})}{\eta_{pump}\eta_{em}}. \quad (6)$$

4.3. Mixing valve/pump and anti-over-pressure droop

As already mentioned in the hypotheses above, a mixing pump has been used in lieu of a valve. This choice has been made with the objective of ensuring the model numerical stability, as in Open Modelica valves are highly unstable. On the other hand, it is pointed out that the mixing pump operates within an extremely low differential pressure, so that its energy consumption is totally negligible (see (6)). In other words, the mixing pump is practically equivalent to a valve.

In terms of control system, the mixing pump is regulated by a PI, which is equipped with saturation and anti-windup, and acts to maintain the hot-water delivery temperature at $T_{del-ref}$.

Following from the introduction, it is observed that DHSs are not usually designed for a flexible pumping operation. In particular, as the DHSs approaches it peak operating conditions, a decrease in T_{del} could result in an excess of mass flow rate and thus in over-pressure issues.

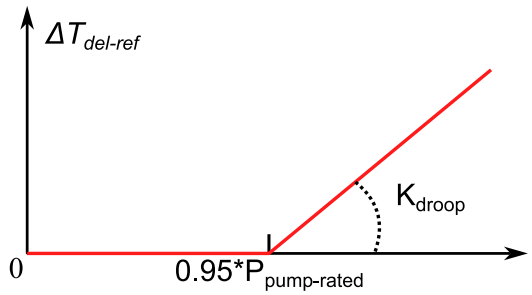

Fig. 5. Over-pressure droop characteristics.

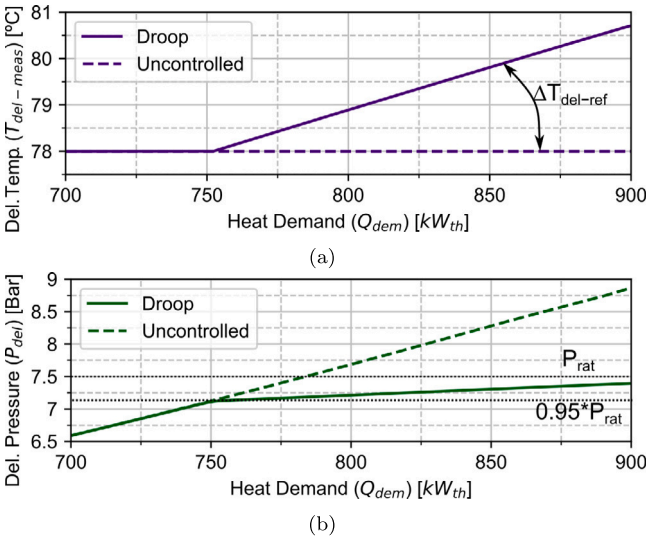

Fig. 6. Over-pressure droop operation: (a) Delivered temperature vs. heat demand, (b) Delivered Pressure vs. heat demand.

To this end, an over-pressure droop is proposed in this work based on the scheme shown in Fig. 4 and the characteristics of Fig. 5.

As it can be seen in Fig. 4, $T_{del-ref}$ is given by the sum of two contributions. The first is the standard set-point $T_{del-ref^0}$, which is set in accordance with the electrical flexibility one wishes to obtain.

The second is the output of the bespoke over-pressure droop control $\Delta T_{del-ref}$. Its operating principle is relatively simple. When the pump pressure is lower than 95% of the rated value $P_{pump-rated}$, the droop output $\Delta T_{del-ref}$ is zero and the system operates normally. Conversely, when 95% of $P_{pump-rated}$ is exceeded the droop kicks in by rising $\Delta T_{del-ref}$. The droop also actuates in conjunction with the limiter of the delivery pump's PI, as the latter impedes that $P_{pump-rated}$ is exceeded, should the droop gain be insufficient.

An example of the anti-over-pressure droop action is shown in Fig. 6, where controlled and uncontrolled conditions are plotted respectively in solid and dashed lines. As it can be seen, when heat demand exceeds 750 kW_{th}, 95% of $P_{pump-rated}$ is reached. Consequently, for larger heat demands, the bespoke droop in engaged that progressively increases the temperature set-point as shown in Fig. 6(a), resulting in a pump pressure curtailment process where $P_{pump-rated}$ is never exceeded, as illustrated in Fig. 6(b).

4.4. Pipes

Hot-water distribution pipes are modelled as a pair of buried pipes, as sketched in Fig. 7(a). In Modelica, this configuration is represented by two heath-exchanging pipes, each of them connected to three thermal resistances, in such a way as to take into account the thermal

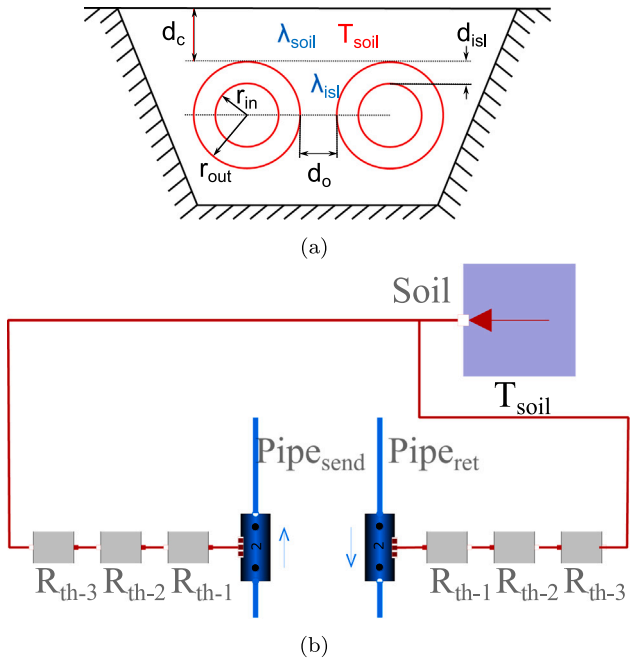

Fig. 7. Pipes modelling: (a) buried pipes, (b) thermal resistances.

losses with the surrounding soil, as shown in Fig. 7(b). The first R_{th-1} represents the thermal resistance of the pipes insulating coat; the second R_{th-2} the soil equivalent thermal resistance, while the third R_{th-3} models the mutual heat exchange. The three resistances are evaluated via (7)–(9), [53], where:

r_{in}: is the pipe internal radius.
r_{out}: is the pipe outer radius.
λ_{isl}: is the insulation thermal conductivity.
L_{pipe}: is the pipe length.
d_c: is the buried depth.
d_o: is the pipes mutual distance.
λ_{soil}: is the soil thermal conductivity.

$$R_{th-1} = \frac{r_{in}\ln(\frac{r_{out}}{r_{in}})}{\lambda_{isl} 4\pi L_{pipe} r_{in}}, \tag{7}$$

$$R_{th-2} = \frac{r_{in}\ln(\frac{4(d_c+r_{out})}{r_{out}})}{\lambda_{soil} 4\pi L_{pipe} r_{in}}, \tag{8}$$

$$R_{th-3} = \frac{r_{in}\ln(\sqrt{(\frac{2(d_c+r_{out})}{d_o+2r_{out}})^2+1})}{\lambda_{soil} 4\pi L_{pipe} r_{in}}, \tag{9}$$

Additionally, in Modelica, the heat transfer between fluid and pipes internal surfaces is also taken into account that is a function of the fluid velocity and hence mass flow rate.

For the DHS of Capriasca, installation and material parameters are reported in Table 3, along with the average soil temperature considered, which has been selected from [54].

4.5. End-users

For each of the nine end-users an equivalent model has been realised based on the assumption that each of them is connected with a temperature-controlled heat exchanger.

Thermal balance within the exchanger can be written as in (10), where superscripts *Pr* and *Sec* denote the primary and secondary sides

Table 3
DHS installation and material parameters.

Parameter	Measure unit	Symbol	Value
Pipes inter-distance	m	d_o	0.2
Pipes buried depth	m	d_c	0.6
Soil thermal conductivity	W/(m K)	λ_{soil}	1.2
Insulation thickness	m	d_{isl}	0.4
Insulation thermal conductivity	W/(m K)	λ_{isl}	0.03
Soil average temperature	°C	T_{soil}	9

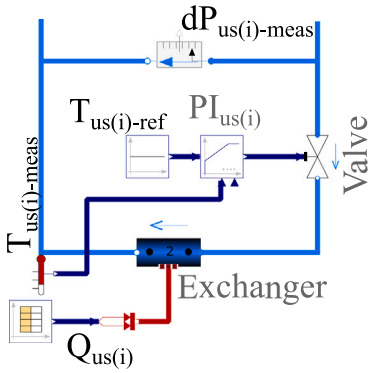

Fig. 8. End-User in Open Modelica.

respectively, while T_{in} and T_{out} are the inlet and outlet temperatures at either side of the exchanger:

$$Q_{us(i)} = \dot{m}^{pr}_{us(i)} c_p (T^{pr}_{in} - T^{pr}_{out}) = \dot{m}^{sec}_{us(i)} c_p (T^{sec}_{in} - T^{sec}_{out}). \tag{10}$$

In the real case, in the secondary circuit, the end-user controller modulates the primary mass flow rate $\dot{m}^{pr}_{us(i)}$ through a valve, in order to maintain T^{sec}_{in} at the set-point value, while $\dot{m}^{sec}_{us(i)}$ is normally constant. Consequently, one may observe that if $\dot{m}^{pr}_{us(i)}$ and $\dot{m}^{sec}_{us(i)}$ are set, the four temperatures possess only two degrees of freedom. By exploiting this property, the model can be simplified by setting the end-user PI to control T^{pr}_{out} rather than T^{sec}_{in}. In this way, it is possible to model only the primary side of the exchanger, as it is shown in Fig. 8, with considerable advantages in terms of execution time and numerical robustness, whilst maintaining the same exchanger thermal energy balance.

In Open Modelica, the end-user is modelled as in Fig. 8. The primary of the heat exchanger is modelled as a heat exchanging pipe, whose outlet temperature $T_{us(i)-meas}$ is controlled by the $PI_{us(i)}$, which regulates the valve opening.

5. The capriasca case study: Analysis methodology

In a bid to provide a thorough yet insightful techno-economic analysis of the proposed idea, three main groups of simulations are conducted:

- A preparatory multi-static analysis.
- Participation in a LFM.
- Participation in a DR Program.

5.1. Preparatory multi-static analysis

In the multi-static analysis, a multitude of steady-state points is obtained. In particular, two characteristics are evaluated:

1. Pumps electricity consumption P_{el} vs. Q_{dem}.
2. Pipes thermal losses Q_{loss} vs. Q_{dem}.

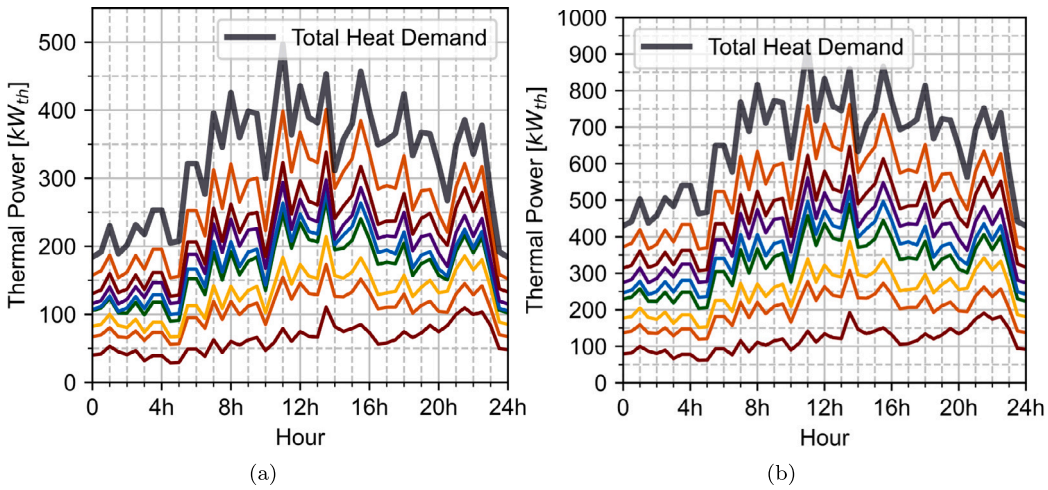

Fig. 9. Heat demand curves of the nine users stacked onto one another and total demand: (a) Typical winter day, (b) Heavy winter day.

In this case, with the objective of getting some qualitative yet valuable information needed to better understand the following two groups of simulations, a direct correlation between P_{el}, Q_{loss} and Q_{dem} is obtained. In particular, for the purpose at hand, dependency of Q_{dem} from time is removed by assuming it to be shared among all end-users proportionally to their rated thermal powers. Then, the two characteristics at hand are evaluated for three values of $T_{del-ref}$, namely 78 °C, 82 °C and 88 °C, corresponding respectively to the maximum, baseline and minimum electricity consumption. Temperature limits have been chosen based on the expertise and recommendations of the DHS operator Capriasca Calore SA.

5.2. Participation in a LFM

In the case of the Capriasca DHS, the existence of an LFM is assumed in order to analyse the potential the DHS possesses. One of the main points to observe is that flexibility changes with the thermal demand, which, in turn, depends on the weather conditions. Therefore, LFM participation is analysed in a typical winter day, where only the wood-fired boiler is engaged, as well as in a heavy winter day, where also the oil-fired one is switched on. Heat consumption for the two winter days is considered for 24 h with a granularity of 30 min. Aggregated consumption derives directly from on-field measurements, whereas individual consumption is estimated based on Authors' expertise and similarity with other DHSs. Fig. 9 illustrates the aggregated and individual heat demands stacked onto one another for the typical and heavy winter day.

In order to assess the DHS participation in a LFM, the following five characteristics are evaluated:

1. Pumps electricity consumption P_{el} vs. time.
2. Upwards flexibility, ϕ_{up}, vs. time.
3. Pipes thermal losses Q_{loss} vs. time.
4. Differential fuel cost Δc_{fuel} vs. time.
5. MMB vs. time.

By observing that LFMs only trade upwards flexibility, the bespoke characteristics are evaluated for both 82 °C and 88 °C, corresponding respectively to the baseline and maximum upwards flexibility.

In accordance with (1), ϕ_{up} is defined as:

$$\phi_{up}(t) = P_{el}(t)\big|_{88\ ^\circ C} - P_{el}(t)\big|_{82\ ^\circ C}. \tag{11}$$

Per-unit values of flexibility are also calculated that are referred to the pumping system rated power.

When it comes to the MMB, LFM is assumed to operate in an hourly basis, i.e., flexibility is traded in hourly packages, so that Δc_{fuel} corresponds to the additional fuel cost for the DHS operator for a 1-hour flexibility package. Subsequently, by recalling the way boilers, tank and their control are modelled, for the generic jth hour, $\Delta c_{fuel(j)}$ can be expressed as follows:

$$\Delta c_{fuel(j)} = \pi_{wood} \int_{t_{(j-1)}}^{t_{(j)}} Q_{wood}(t)\big|_{88\ ^\circ C} - Q_{wood}(t)\big|_{82\ ^\circ C}\, dt + \pi_{oil} \int_{t_{(j-1)}}^{t_{(j)}} Q_{oil}(t)\big|_{88\ ^\circ C} - Q_{oil}(t)\big|_{82\ ^\circ C}\, dt, \tag{12}$$

where $t_{(j-1)}$ and $t_{(j)}$ represent the first and last time instants of the jth hour, while π_{wood} and π_{oil} are the wood and oil prices, whose values are reported in Table 4. Eventually, to fully assess the MMB, it is also necessary to take into account the variation in electricity cost Δc_{el}. In an analogous manner to (12), for the generic jth hour, $\Delta c_{el(j)}$ can be expressed as in (13), where π_{el} is assumed to be constant during the jth hour:

$$\Delta c_{el(j)} = \pi_{el} \int_{t_{(j-1)}}^{t_{(j)}} P_{el}(t)\big|_{88\ ^\circ C} - P_{el}(t)\big|_{82\ ^\circ C}\, dt. \tag{13}$$

As a result, the MMB can be defined as:

$$MMB_{(j)} = \Delta c_{fuel(j)} + \Delta c_{el(j)}. \tag{14}$$

Following from (13), LFM participation analysis is conducted for five different electricity prices, namely 0.03 €/kWh, 0.06 €/kWh, 0.09 €/kWh, 0.15 €/kWh and 0.24 €/kWh. These values have been chosen in a bid to represent different forms of access to the electricity, ranging from self-consumption solutions (low prices) to traditional retail markets (high prices).

Table 4
Wood and oil prices.

	Wood	Oil
Price (π) [€/kWh]	0.06	0.10

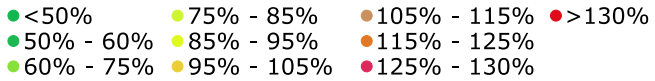

Fig. 10. Capriasca distribution grid congestion level colour code.

5.3. Participation in a demand response program

As already mentioned in Section 2.3.3, DR mechanisms are activated in order to solve contingent or foreseen technical issues in distribution

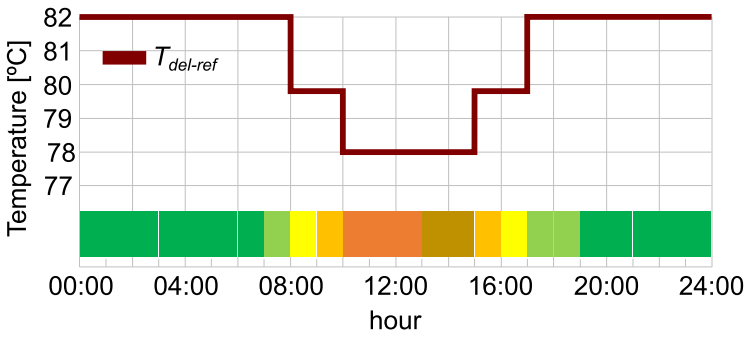

Fig. 11. Capriasca distribution grid load level and $T_{del-ref}$.

grids. In order to correlate these issues with a DR intervention request, in this work, the so-called traffic-light approach is used. The load level of the transformer serving the Capriasca distribution grid is considered as critical indicator and different colours are assigned to different load levels, as represented in Fig. 10. Then, based on the traffic light colour, different DR requests are generated. Subsequently, a grid scenario is defined where a considerable overload is found in the Capriasca's distribution transformer. The load daily profile is depicted in the colour bar of Fig. 11, with an overload being experienced between 10 a.m. and 3 p.m. At this point, an assumption is made that the overload is caused by an excess of distributed generation in the grid and a DR mechanism is defined with the following flexibility requests:

- 50% downwards flexibility between 95% and 105% load (8 a.m. to 10 a.m. and 3 p.m. to 5 p.m.).
- 100% downwards flexibility above 105% load (10 a.m. to 3 p.m.).

Theoretically, translating the 50% and 100% flexibility requests into a temperature setpoint would require a relatively complex process that would be out of the scope of this work. As an alternative, a simplified approach is used in this example. By analysing the results of the preparatory multi-static analysis (shown later in Section 6.1), a quadratic relation between the hot water delivery temperature and flexibility is found. Then, by keeping the same temperature range used for the LFM analysis, a 79.8 °C and 78 °C set-points are selected for the 50% and 100% downwards flexibility respectively, as shown in Fig. 11.

At this point, given that the DR event begins at t_i and ends at t_f, the Minimum Acceptable Token (MAT) can be defined. Here, it is important to highlight that several token options are currently being proposed in the literature [5]. In this example, tokens are assumed to be a "one-shot" electricity price π_{el}^{DR} that supersedes the initial price π_{el}^{0} for the whole duration of the DR event. Based on that, the overall energy cost of participating in the DR event needs to be lower than in the baseline condition:

$$\pi_{fuel}\ E_{fuel}\big|_{T^{DR}_{del-ref}} + \pi_{el}^{DR}\ E_{el}\big|_{T^{DR}_{del-ref}} < \pi_{fuel}\ E_{fuel}\big|_{82\ ^\circ\mathrm{C}} + \pi_{el}^{0}\ E_{el}\big|_{82\ ^\circ\mathrm{C}} \quad (15)$$

where:

$$\pi_{fuel}\ E_{fuel}\big|_{T^{DR}_{del-ref}} = \pi_{wood} \int_{t_i}^{t_f} Q_{wood}(t)\big|_{T^{DR}_{del-ref}}\, dt + \pi_{oil} \int_{t_i}^{t_f} Q_{oil}(t)\big|_{T^{DR}_{del-ref}}\, dt, \quad (16)$$

$$\pi_{el}^{DR}\ E_{el}\big|_{T^{DR}_{del-ref}} = \pi_{el}^{DR} \int_{t_i}^{t_f} P_{el}(t)\big|_{T^{DR}_{del-ref}}\, dt, \quad (17)$$

$$\pi_{fuel}\ E_{fuel}\big|_{82\ ^\circ\mathrm{C}} = \pi_{wood} \int_{t_i}^{t_f} Q_{wood}(t)\big|_{82\ ^\circ\mathrm{C}}\, dt + \pi_{oil} \int_{t_i}^{t_f} Q_{oil}(t)\big|_{82\ ^\circ\mathrm{C}}\, dt, \quad (18)$$

$$\pi_{el}^{0}\ E_{el}\big|_{82\ ^\circ\mathrm{C}} = \pi_{el}^{0} \int_{t_i}^{t_f} P_{el}(t)\big|_{82\ ^\circ\mathrm{C}}\, dt, \quad (19)$$

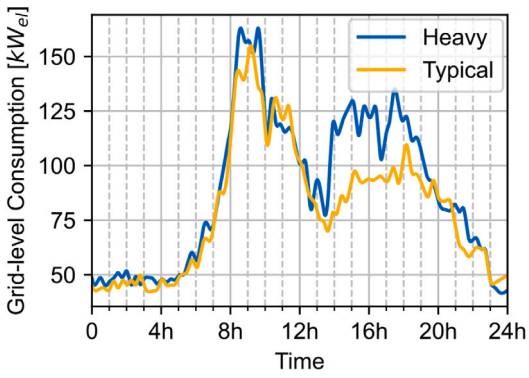

Fig. 12. DHS users electric demand in a typical and heavy winter day.

Consequently, the MAT can be found by equalling the two terms in (15) and solving for π_{el}^{DR}:

$$MAT = \frac{\pi_{fuel}\ E_{fuel}\big|_{82\ ^\circ\mathrm{C}} + \pi_{el}^{0}\ E_{el}\big|_{82\ ^\circ\mathrm{C}} - \pi_{fuel}\ E_{fuel}\big|_{T^{DR}_{del-ref}}}{E_{el}\big|_{T^{DR}_{del-ref}}} \quad (20)$$

The DR participation analysis is conducted with three main objectives. Firstly, to quantify the MAT in a typical and heavy winter day. Secondly, to compare the flexibility contribution of the DHS against the overall electric consumption of its users. Thirdly, to observe the impact of the droop control. In order to assess the bespoke objectives, the following characteristics are evaluated:

1. Pumps electricity consumption P_{el} vs. time,
2. Downwards flexibility ϕ_{do} vs. time,
3. Pipes thermal losses Q_{loss} vs. time,
4. Grid-level downwards flexibility γ_{do} vs. time, where γ_{do} indicates the ratio (in %) between ϕ_{do} and the overall DHS users electric demand. This last is plotted in Fig. 12.
5. MAT vs. original electricity price π_{el}^{0}.

With regards of Fig. 12, it is observed that a small variation of the transformer load is incurred, so that the same profile shown in Fig. 11 is used for both cases. In general terms, DR mechanisms are expected to operate for both downwards and upwards flexibility. On the other hand, in the case of this work, the upwards one has been already analysed in the LFM case. Therefore, to keep this manuscript within a reasonable length, downwards flexibility only is now taken into account.

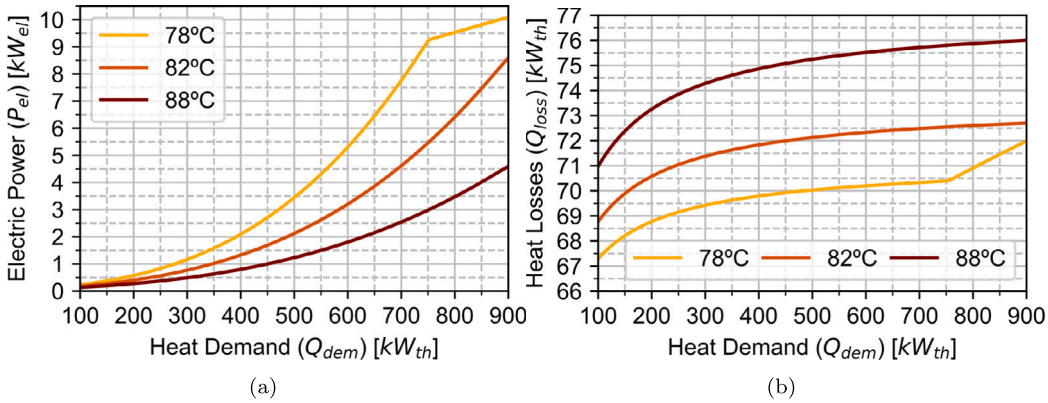

Fig. 13. Multi-static analysis results: (a) Electric power, (b) Pipes losses.

6. The capriasca case study: Results and discussion

6.1. Preparatory multi-static analysis

Multi-static analysis results are illustrated in Fig. 13(a)–(b). From 13(a) one may see that P_{el} follows a nonlinear trend against Q_{dem}, which can be demonstrated to be approximable with a cubic polynomial. Additionally, the power curtailment due to the over-pressure droop is observable at 750 kWh_{th} in the 78 °C curve.

For what is concerned with heat losses, a nonlinear trend is also observed. Here, a relatively high growth rate in the low Q_{dem} region and an almost flat shape at high Q_{dem} are found. This trend stems from the different heat transfer coefficient between fluid and pipe at different fluid velocities, i.e., mass flow rates, which is taken into account by the Modelica model.

6.2. Participation in a LFM

Results obtained for the typical and heavy winter day are illustrated in Figs. 14(a)–(d), 15, 16(a)–(d) and 17.

In the typical winter day, as shown in Fig. 14(b), flexibility between −0.5 kW_{el} and −1 kW_{el} is available for all morning hours, with the peak value reached at 11 a.m. corresponding to the highest Q_{dem}. In terms of percent values, 30% to 40% values are available throughout the entire day. Eventually, in terms of Δc_{fuel}, it is observed that the highest Δc_{fuel} does not correspond to the highest flexibility. In fact, Δc_{fuel} is related to the difference in Q_{loss} at different operating temperatures, which occurs during the dip in consumption taking place at 2 p.m., as Q_{loss} possesses a higher variation rate against Q_{dem} (see Fig. 13).

MMB results are shown in Fig. 15. As it can be seen, the lowest $MMBs$ are obtained for the highest π_{el}, as operating at a higher temperatures reduces the electricity consumption, resulting in higher economic savings. Conversely, when π_{el} is extremely low, i.e., 0.03 €/kWh, the MMB is practically equal to the differential fuel cost Δc_{fuel}. All the above provides an insightful example of the way SC works. In simple words, given that the fuel price is constant, the higher π_{el} the more the convenience in shifting energy from the electric to the thermal vector.

For the heavy winter day, results are shown in Fig. 16(a)–(d), while the MMB is illustrated in Fig. 17. Here, the first point to note is concerned with the variation of flexibility, losses and Δc_{fuel}. In fact, as heat demand exceeds 700 kWh for several hours, the general trend of Fig. 13 shows that variations in Q_{dem} result in considerable variations of P_{el}, whereas Q_{loss} remain almost constant. As a result, flexibility peaks at −3.5 kW, which is 2.3 times higher than in a typical day, although the peak in Δc_{fuel} increases of only 1.1 times. For what is concerned the MMB, it is critical to observe that negative values are obtained when π_{el} is higher than 0.15 €/kWh. This fact results from the same behaviour described above, i.e., a considerable increase in electricity consumption against an almost negligible variation in heat loss. Consequently, in case of high electricity prices, Δc_{el} can exceed Δc_{fuel}. In other words, the analysis conducted in this work to investigate DHS flexibility-related aspects shows that the "baseline" might not be optimal for heavy weather conditions, as negative $MMBs$ indicate that an increase in temperature would be economically beneficial regardless of flexibility purposes. In accordance with the above, it should be pointed out that it is not unusual for DHS operators to increase $T_{del-ref}$ in case of heavy weather conditions and high electricity prices. For what is concerned with this work, setting a new $T_{del-ref}$ would mean to recalculate the baseline consumption based on an optimisation process, which would be out of scope.

6.3. Participation in a DR program

Results obtained for the typical and heavy winter day are illustrated in Figs. 18(a)–(d), 19, 20(a)–(e) and 21. This time the spotlight of attention is on the downwards flexibility.

In the typical winter day, flexibility values between 0.5 kW_{el} and 1.5 kW_{el} are obtained, corresponding to percent values between 25% and 60%, with the peak being reached once again in correspondence with the peak thermal demand at 11 a.m. As expected, in Fig. 18(a) no intervention of the droop controller can be seen. Eventually, Fig. 18(d) shows the relatively low contribution of the DHS to the overall electric consumption of the nine users, as γ_{do} ranges between 0.20% and 1.25%. In Fig. 19, the MAT is shown along with $\Delta\pi_{el}$, this last being defined as the minimum acceptable electricity price variation with respect to the MAT:

$$\Delta\pi_{el} = MAT - \pi^0_{el}. \tag{21}$$

Firstly, one can note that MAT grows proportionally to π^0_{el}. However, more insightful considerations can be done with respect to $\Delta\pi_{el}$, which becomes negative for π^0_{el} of around 0.205 €/kWh. This, in turn, shows that at relatively low electricity prices the energy savings obtained from the reduction in fuel consumption attained during the DR event would compensate even for an increase in the electricity price. Conversely, for initial electricity prices higher than 0.205 €/kWh, a discount is required to make DR request economically viable. This aspect is commented further in Section 6.4.

In the heavy winter day, flexibility considerably grows, as values between 1.5 kW_{el} and 3.5 kW_{el} are obtained, corresponding to extremely high percent values between 30% and 70%. Additionally, it should be noted that the peak value is also curtailed by the engagement of the anti-over-pressure droop, whose intervention is visible in the rounded peak shape, as well as in Fig. 20(e). For what is concerned with the contribution to the overall electric consumption of the nine users, γ_{do} still remains as low as 1% to 3%. Regarding the MAT and $\Delta\pi_{el}$, this last becomes negative at an initial electricity price as low as 0.08 €/kWh, so that a discount is almost always necessary to make DR participation economically convenient.

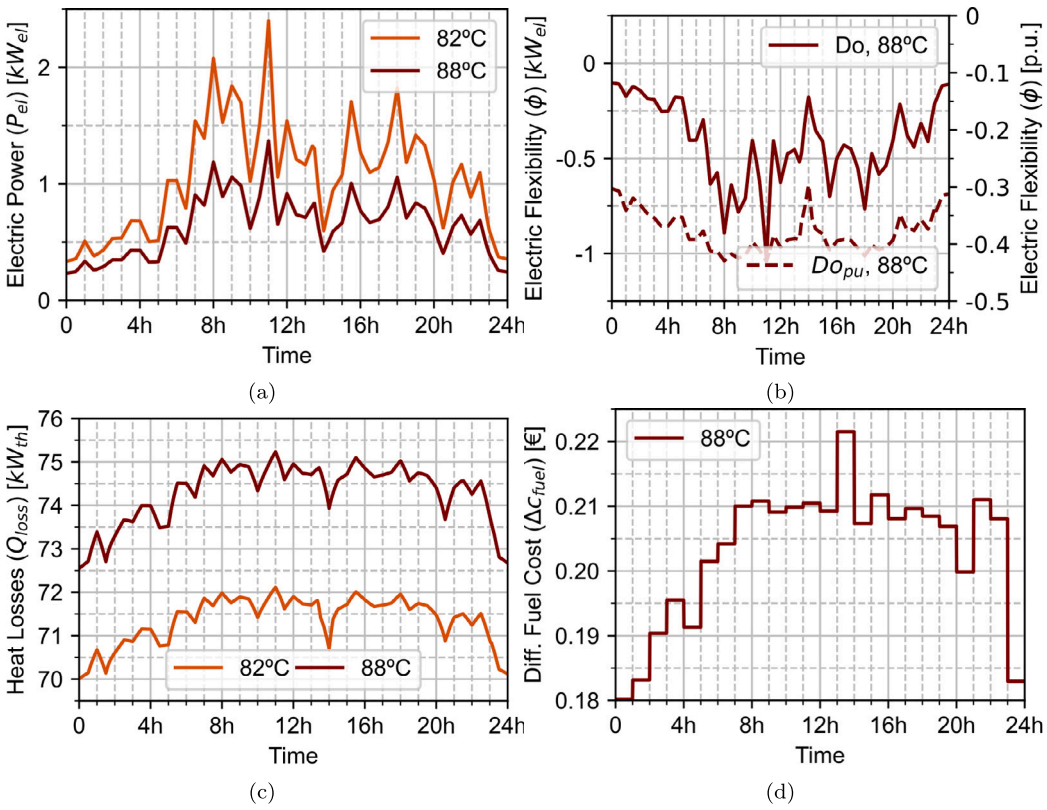

Fig. 14. LFM analysis in a typical winter day: (a) Electric power, (b) Upwards flexibility, (c) Pipes losses, (d) Differential fuel cost.

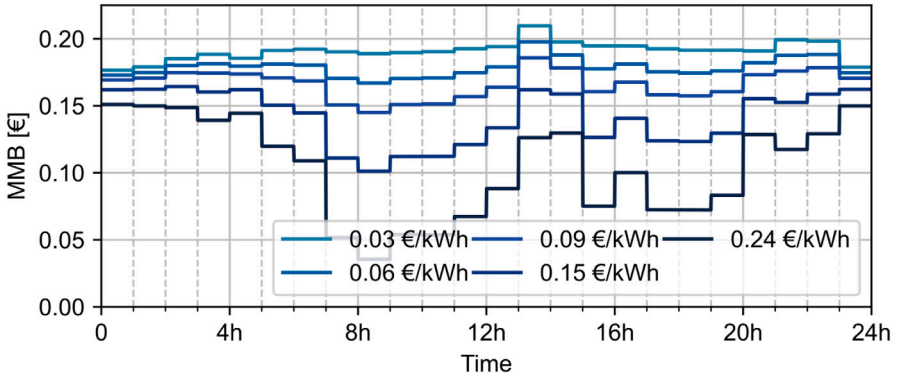

Fig. 15. LFM analysis in a typical winter day: MMB.

6.4. Results discussion

Following from the results obtained and presented in the previous subsections, the key findings are discussed below.

In terms of available flexibility, a twofold consideration need to be made. In terms of absolute values, available flexibility depends on the overall pumping power installed, which is usually one or more orders of magnitude lower than the thermal power. In this work, relatively low absolute flexibilities are obtained, with a maximum of 3.5 kW. This, in turn, resulted in a relatively low contribution in changing the overall electricity consumption of the nine users, as variations of up to 3% are attained. On the other hand, very high percent flexibility values are reached, ranging from 25% to 70%, which is comparable with a Battery Energy Storage (BES) or an EV charger. From the above, it is concluded that DHSs possess a good potential to provide flexibility services, which could be of special interest for very large DHSs counting on tens of kWs of pumping powers.

To continue the comparison between DHSs and conventional flexible loads such as BESs, EVs or HPs, the second key variable needs to be acknowledged, i.e., time. In fact, in BESs and EVs, flexibility is available for a limited time period depending on the State of Charge (SoC). Similarly, for HPs, flexibility time depends on the thermal energy needed to meet the users comfort. Conversely, in DHSs, flexibility is obtained by shifting energy between the thermal and electric vectors, which has no time limitation. In other words, DHSs flexibility is available for unlimited time periods.

By comparing now downwards and upwards flexibility of DHSs, Fig. 13(a) shows that the former is higher than the latter for the same Q_{dem}. By observing (5), one may see that for the same Q_{dem} temperature and mass flow rate are linearly proportional, whereas it is well known that hydraulic losses change quadratically against the flow rate, and so does the electricity consumption.

As pointed out in Sections 6.2 and 6.3, downwards and upwards flexibility show a considerable variation against the thermal demand. Consequently, as already anticipated in Section 5.3, development of

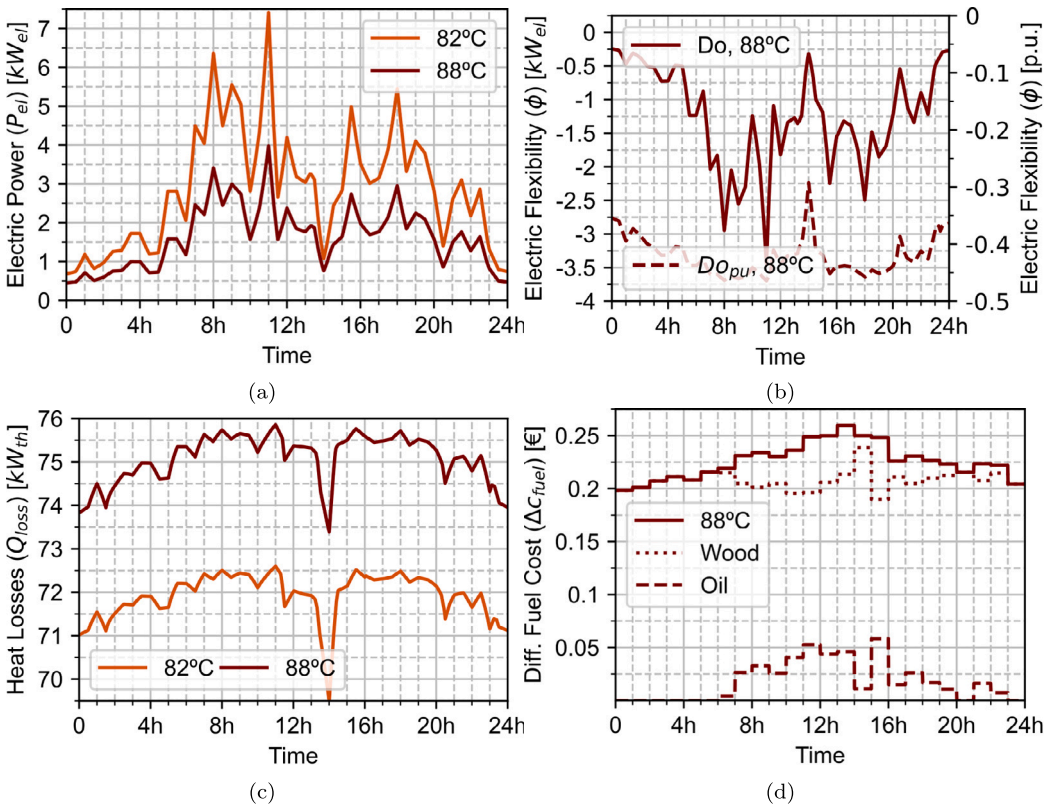

Fig. 16. LFM analysis in a heavy winter day: (a) Electric power, (b) Upwards flexibility, (c) Pipes losses, (d) Differential fuel cost.

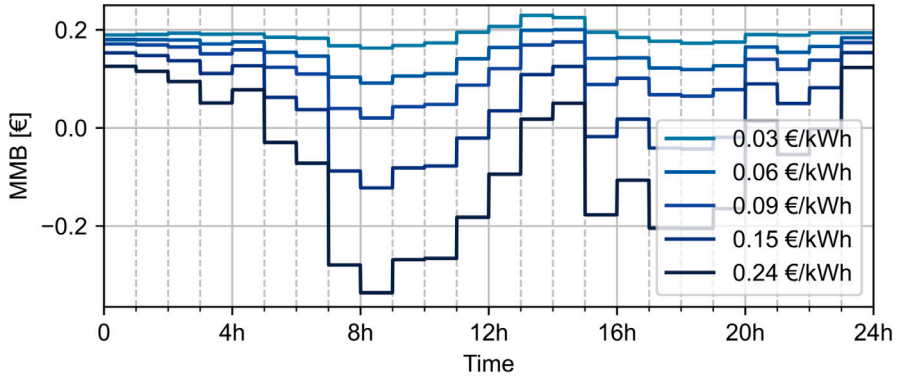

Fig. 17. LFM analysis in a heavy winter day: MMB.

advanced control systems would be necessary in order to adjust $T_{del-ref}$ in such a way as to get the desired flexibility value.

From the economic perspective, the first point to note is that the implementation of the proposed idea of changing $T_{del-ref}$ based on the desired flexibility does not require the installation of new devices, as it only needs an updated control logic. Therefore, implementation costs are negligible. In terms of economic benefits, both MMB and MAT showed two main points: (i) the economic viability of a flexible DHS operation, and (ii) the strong bonding between MMB/MAT and electricity prices. With regards to the latter, low electricity prices represent cheap energy scenarios, such as individual or shared self-consumption (a local energy community), etc. Thus, MMB/MAT results show the strong economic synergy between low electricity prices and participation in LFMs and DR schemes, which, in turn, demonstrates the additional advantages for DHS operators in investing in self-consumption solutions. Additionally, results point out that it would be worth considering the additional incomes of flexible operation even in the design process of future DHSs. Indeed, the extra cost of a more powerful pumping system could be more than compensated by the participation in LFMs and DR schemes. Here, it is worth observing that nowadays there exist very few examples of real LFMs, so that predicting the actual revenue streams for participation remains a highly complex task.

Eventually, the negative MMB values observed in Fig. 17, together with the positive MAT found for low electricity prices indicate that the traditional control scheme with a constant $T_{del-ref}$ does not optimise the overall fuel plus electricity cost. Consequently, by taking into account the higher volatility expected for electricity prices, it would be worth developing a more advanced control strategy where $T_{del-ref}$ is changed with the objective of minimising the overall energy cost.

The final point to note is concerned with the simplifying hypotheses the model proposed in this work is based on. As confirmed by the results, these last are suitable for the purposes of a techno-economic

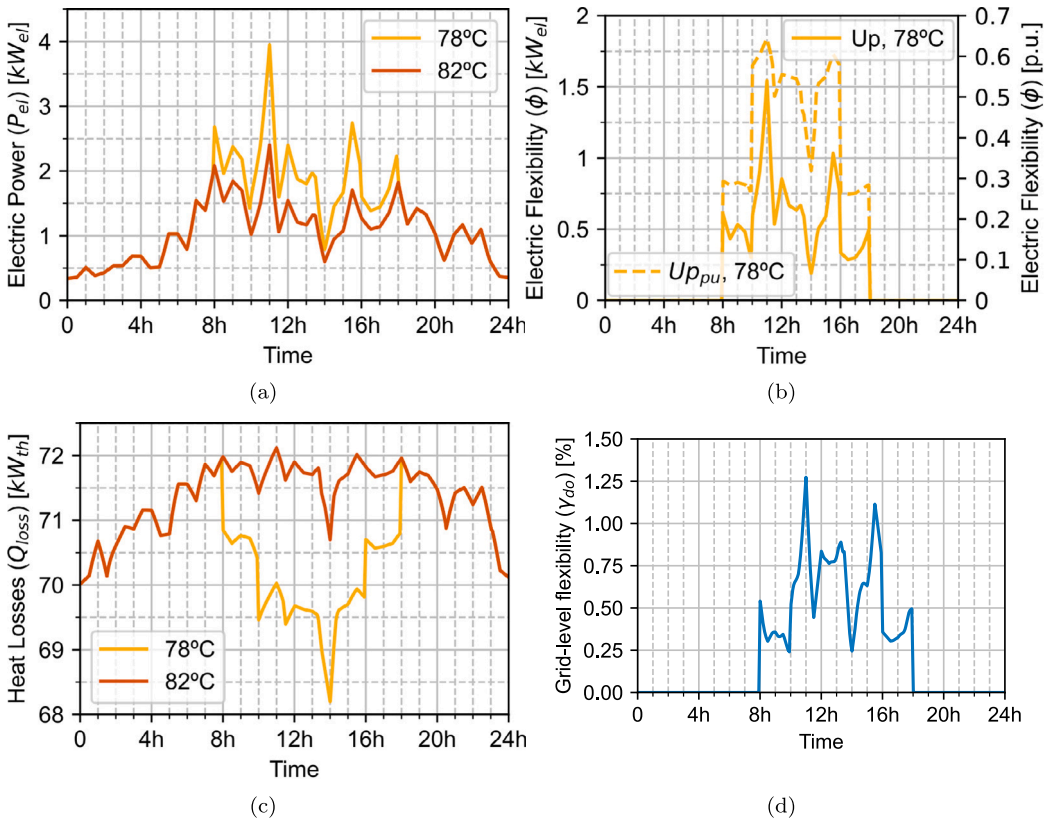

Fig. 18. DR analysis in a typical winter day: (a) Electric power, (b) Downwards flexibility, (c) Pipes losses, (d) Grid-level downwards flexibility.

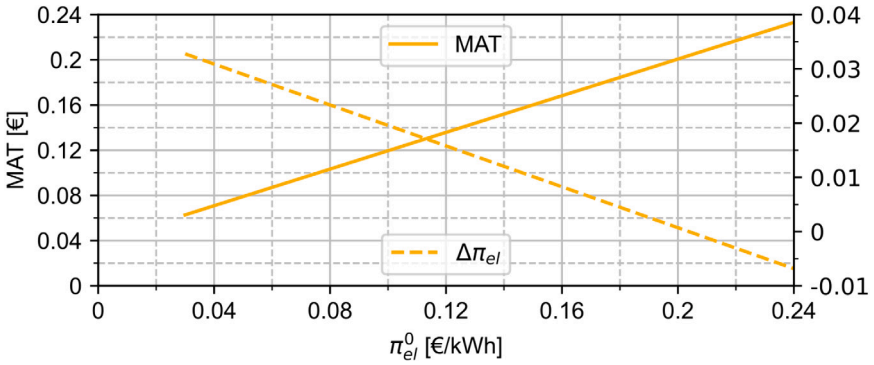

Fig. 19. DR analysis in a typical winter day: MAT and $\Delta\pi_{el}$.

analysis. On the other hand, dynamics of transient phenomena might not be accurately assessed, so that development more accurate simulation models and/or experimental setups represents a key part for future works.

7. Conclusion

This work has proposed an alternative control strategy for combustion-based DHSs allowing the pumping system to operate as a flexible load. The idea has been conducted in the case study of Capriasca (Lugano), where a techno-economic analysis has been conducted considering participation in a LFM and in a DR program. The key findings have been reported and discussed in Section 6.4 and can be summarised as follows:

- Very high percent flexibility values are reached, in the range between 25% and 70%, although absolute flexibility values are limited by the rated pumping power, making flexible operation especially attractive for very large DHSs.
- As opposed to conventional electric loads, DHSs can provide flexibility for potentially unlimited time periods.
- Available flexibility depends on the thermal demand, so that advanced control strategies are needed to obtain the desired flexibility.
- If downwards flexibility is desired, over pressure issues needs to be avoided. This work proposed a pressure vs. temperature droop controller, which proved to be simple yet effective.
- From the economic perspective, the additional advantages of flexible operation have been shown, especially in very low electricity price scenarios.
- Given the expected volatility of future electricity prices, DHSs flexible operation should be considered for both DHSs design and optimal dispatch.

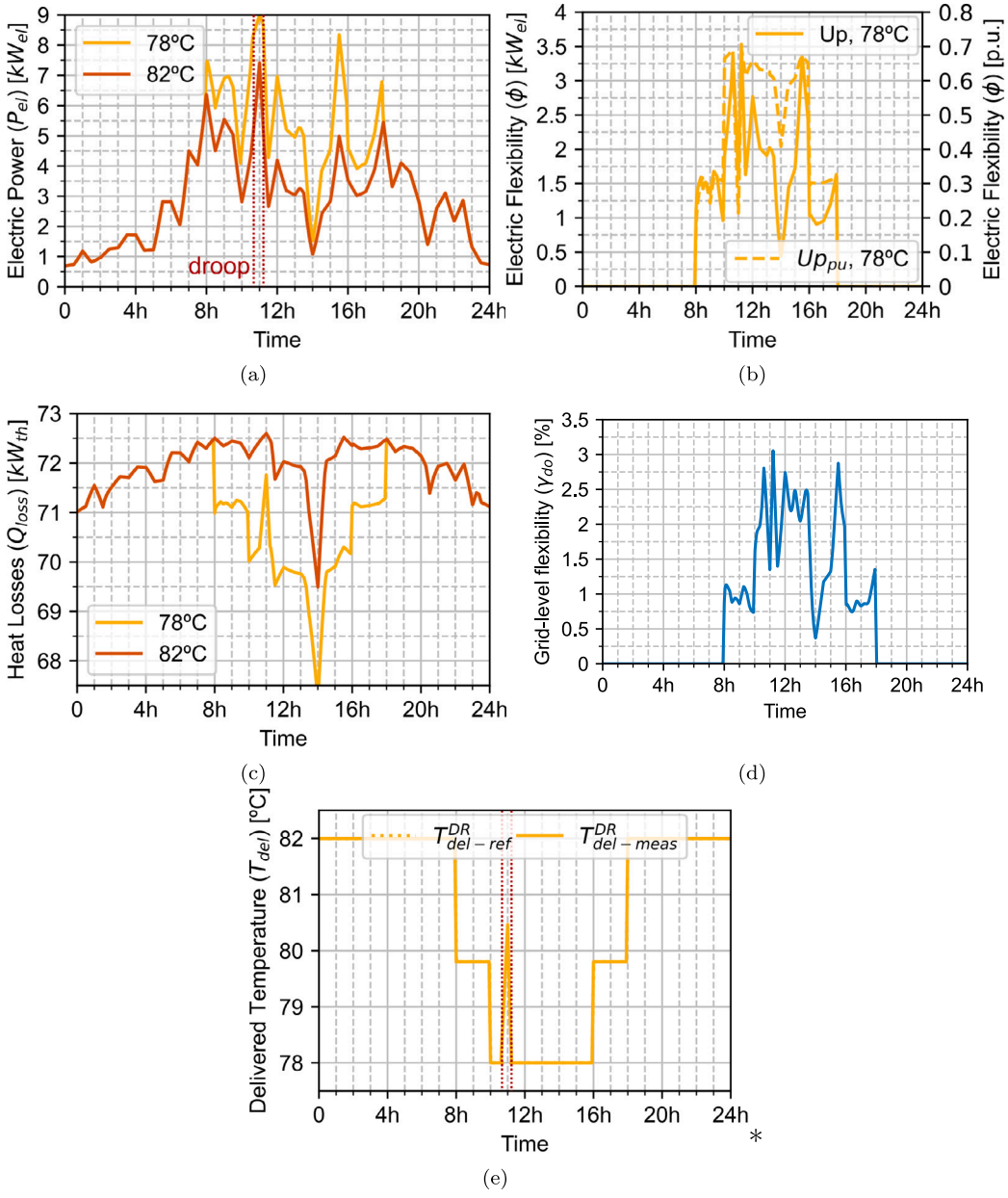

Fig. 20. DR analysis in a heavy winter day: (a) Electric power, (b) Downwards flexibility, (c) Pipes losses, (d) Grid-level downwards flexibility, (e) Anti-over-pressure droop.

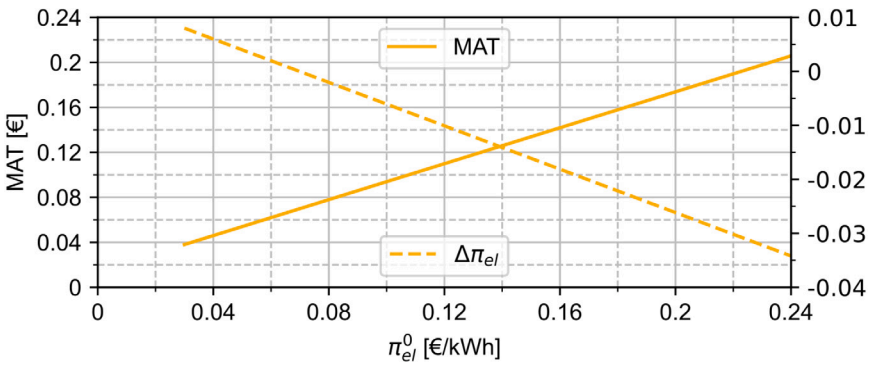

Fig. 21. DR analysis in a heavy winter day: MAT and $\Delta\pi_{el}$.

CRediT authorship contribution statement

Roberto Rocca: Conception and design of study, Acquisition of data (laboratory or clinical), Data analysis and/or interpretation, Writing – original draft, Writing – review & editing. **Lorena Elorza-Uriarte:** Conception and design of study, Acquisition of data (laboratory or clinical), Data analysis and/or interpretation, Writing – original draft, Writing – review & editing. **Itziar Zubia:** Conception and design of study, Data analysis and/or interpretation, Writing – original draft, Writing – review & editing. **Daniele Farrace:** Conception and design of study, Data analysis and/or interpretation. **Riccardo Toffanin:** Conception and design of study, Acquisition of data (laboratory or clinical), Data analysis and/or interpretation, Writing – original draft, Writing – review & editing. **David Miguel Rivas-Ascaso:** Conception and design of study, Data analysis and/or interpretation.

Declaration of competing interest

The authors declare that they have no known competing financial interests or personal relationships that could have appeared to influence the work reported in this paper.

Data availability

The authors do not have permission to share data.

Acknowledgements

This work has been developed within the framework of the H2020 - ACCEPT project, which has received funding from the European Union's Horizon 2020 research and innovation programme under grant agreement No 957781. Authors wish to express their gratitude to Capriasca Calore SA, Reglasystem SA and Azienda Elettrica di Massagno (AEM) SA for their technical support and the provision of real aggregated consumption data. All authors approved the version of the manuscript to be published.

References

[1] European C. European green deal. 2019, URL https://commission.europa.eu/strategy-and-policy/priorities-2019-2024/european-green-deal_en.

[2] Surve SP, Rocca R, Engeveld EJ, Martínez D, Comech MP, Rivas DM. Impact assessment of different battery energy storage technologies in distribution grids with high penetration of renewable energies. Renew Energy Power Qual J (RE&PQJ) 2022;20:650–5. http://dx.doi.org/10.24084/repqj20.391.

[3] Menéndez-Agudín A, Rocca R, Fernández G, Luengo-Baranguán L, Zaldivar D. Hydrogen technologies to provide flexibility to the electric system: A review. Renew Energy Power Qual J (RE&PQJ) 2022;20:656–61. http://dx.doi.org/10.24084/repqj20.392.

[4] Rocca R, Papadopoulos S, Rashed M, Prassinos G, Giulii Capponi F, Galea M. A one-body, laminated-rotor flywheel switched reluctance machine for energy storage: Design trade-offs. In: 2020 IEEE international conference on environment and electrical engineering and 2020 IEEE industrial and commercial power systems europe. EEEIC/I&CPS Europe, IEEE; 2020, p. 1–6. http://dx.doi.org/10.1109/EEEIC/ICPSEurope49358.2020.9160512.

[5] Morales-España G, Martínez-Gordón R, Sijm J. Classifying and modelling demand response in power systems. Energy 2022;242:122544. http://dx.doi.org/10.1016/j.energy.2021.122544.

[6] Loschan C, Schwabeneder D, Lettner G, Auer H. Flexibility potential of aggregated electric vehicle fleets to reduce transmission congestions and redispatch needs: A case study in Austria. Int J Electr Power Energy Syst 2023;146:108802. http://dx.doi.org/10.1016/j.ijepes.2022.108802.

[7] Junaidi N, Abdullah MP, Alharbi B, Shaaban M. Blockchain-based management of demand response in electric energy grids: A systematic review. Energy Rep 2023;9:5075–100. http://dx.doi.org/10.1016/j.egyr.2023.04.020.

[8] Kerscher S, Arboleya P. The key role of aggregators in the energy transition under the latest European regulatory framework. Int J Electr Power Energy Syst 2022;134:107361. http://dx.doi.org/10.1016/j.ijepes.2021.107361.

[9] Ostovar S, Moeini-Aghtaie M, Hadi MB. Designing a new procedure for participation of prosumers in day-ahead local flexibility market. Int J Electr Power Energy Syst 2023;146:108694. http://dx.doi.org/10.1016/j.ijepes.2022.108694.

[10] Chantzis G, Papadopoulos AM, Giama E, Nizetic S. The potential of demand response as a tool for decarbonization in the energy transition. Energy Build 2023;113255. http://dx.doi.org/10.1016/j.enbuild.2023.113255.

[11] Shen F, Wu Q, Jin X, Zhang M, Teimourzadeh S, Tor OB. Coordination of dynamic tariff and scheduled reprofiling product for day-ahead congestion management of distribution networks. Int J Electr Power Energy Syst 2022;135:107612. http://dx.doi.org/10.1016/j.ijepes.2021.107612.

[12] Zhang C, Wang Q, Wang J, Korpås M, Khodayar ME. Strategy-making for a proactive distribution company in the real-time market with demand response. Appl Energy 2016;181:540–8. http://dx.doi.org/10.1016/j.apenergy.2016.08.058.

[13] Sørensen ÅL, Lindberg K, Sartori I, Andresen I. Analysis of residential EV energy flexibility potential based on real-word charging reports and smart meter data. Energy Build 2021;241:110923. http://dx.doi.org/10.1016/j.enbuild.2021.110923.

[14] Bernal-Sancho M, Rocca R, Fernández-Aznar G, Comech MP, Galán-Hernández N. Grid impact of frequency regulation provided by V2Gs aggregated at HV, MV, and LV level. IEEE Access 2023;11:76768–80. http://dx.doi.org/10.1109/ACCESS.2023.3296220.

[15] Mimica M, Boras I-P, Krajacic G. The integration of the battery storage system and coupling of the cooling and power sector for increased flexibility under the considerations of energy and reserve market. Energy Convers Manage 2023;286:117005. http://dx.doi.org/10.1016/j.enconman.2023.117005.

[16] Arabzadeh V, Mikkola J, Jasiunas J, D.Lund P. Deep descarbonization of urban energy systems through renewable energy and sector-coupling flexibility strategies. J Environ Manag 2020;260(110090). http://dx.doi.org/10.1016/j.jenvman.2020.110090.

[17] Fleschutz M, Bohlayer M, Braun M, D.Murphy M. From prosumer to flexumer: Case study on the value of flexibility in descarbonizing the multi-energy system of a manufacturing company. Appl Energy 2023;347(121430). http://dx.doi.org/10.1016/j.apenergy.2023.121430.

[18] Rinaldi A, Christoph Soini M, Streicher K, K. Patel M, Parra D. Decarbonising heat with optimal PV and storage investments: A detailed sector coupling modelling framework with flexible heat pump operation. Appl Energy 2021;282(116110). http://dx.doi.org/10.1016/j.apenergy.2020.116110.

[19] Khalkhali H, Hossein Hosseinian S. Tapping on the aggregate flexibility of heterogeneous load groups for EV fast charge accommodation in urban power distribution networks. Sustainable Cities Soc 2021;74(103169). http://dx.doi.org/10.1016/j.scs.2021.103169.

[20] Fernqvist N, Broberg S, Torén J, Svensson I-L. District heating as a flexibility service: Challenges in sector coupling for increased solar and wind power production in Sweden. Energy Policy 2023;173(113332). http://dx.doi.org/10.1016/j.enpol.2022.113332.

[21] Tan K, Wu Q, Zhang M. Strategic investment for district heating systems participating in energy and reserve markets using flexibility. Int J Electr Power Energy Syst 2022;137(107810). http://dx.doi.org/10.1016/j.ijepes.2021.107819.

[22] Schwele A, Arrigo A, Vervaeren C, Kazempour J, Vallée F. Coordination of electricity, heat, and natural gas systems accounting for network flexibility. Electr Power Syst Res 2020;189:106776. http://dx.doi.org/10.1016/j.epsr.2020.106776.

[23] Huang W, Zhang N, Cheng Y, Yang J, Wang Y, Kang C. Multienergy networks analytics: Standardized modeling, optimization, and low carbon analysis. Proc IEEE 2020;108(9):1411–36. http://dx.doi.org/10.1109/JPROC.2020.2993787.

[24] Martínez Ceseña EA, Loukarakis E, Good N, Mancarella P. Integrated electricity–heat–gas systems: Techno–economic modeling, optimization, and application to multienergy districts. Proc IEEE 2020;108(9):1392–410. http://dx.doi.org/10.1109/JPROC.2020.2989382.

[25] Coelho A, Iria J, Soares F. Network-secure bidding optimization of aggregators of multi-energy systems in electricity, gas, and carbon markets. Appl Energy 2021;301:117460. http://dx.doi.org/10.1016/j.apenergy.2021.117460.

[26] Coelho A, Iria J, Soares F, Lopes JP. Real-time management of distributed multi-energy resources in multi-energy networks. Sustain Energy Grids Netw 2023;34:101022. http://dx.doi.org/10.1016/j.segan.2023.101022.

[27] Majidi M, Davoodi E, Li B, Mohammadi-Ivatloo B, Parvania M. Continuous-time day-ahead operation of multienergy systems. IEEE Syst J 2020;15(4):5595–605. http://dx.doi.org/10.1109/JSYST.2020.3035237.

[28] Bashir AA, Jokisalo J, Heljo J, Safdarian A, Lehtonen M. Harnessing the flexibility of district heating system for integrating extensive share of renewable energy sources in energy systems. IEEE Access 2021;9:116407–26. http://dx.doi.org/10.1109/ACCESS.2021.3105829.

[29] Hadachi I, Voss M, Albayrak S. Sector-coupled district energy management with heating and bi-directional EV-charging. In: 2021 IEEE madrid powerTech. IEEE; 2021, p. 1–6. http://dx.doi.org/10.1109/PowerTech46648.2021.9495040.

[30] Liu X, Wu J, Jenkins N, Bagdanavicius A. Combined analysis of electricity and heat networks. Appl Energy 2016;162:1238–50. http://dx.doi.org/10.1016/j.apenergy.2015.01.102.

[31] Cao Y, Wei W, Wu L, Mei S, Shahidehpour M, Li Z. Decentralized operation of interdependent power distribution network and district heating network: A market-driven approach. IEEE Trans Smart Grid 2019;10(5):5374–85. http://dx.doi.org/10.1109/TSG.2018.2880909.

[32] Tan J, Wu Q, Zhang M. Strategic investment for district heating systems participating in energy and reserve markets using heat flexibility. Int J Electr Power Energy Syst 2022;137:107819. http://dx.doi.org/10.1016/j.ijepes.2021.107819.

[33] Yang C, Li Z. Distributed conditional-distributionally robust coordination for an electrical power and flexibility-enhanced district heating system. Appl Energy 2023;347:121491. http://dx.doi.org/10.1016/j.apenergy.2023.121491.

[34] Xu X, Lyu Q, Qadrdan M, Wu J. Quantification of flexibility of a district heating system for the power grid. IEEE Trans Sustain Energy 2020;11(4):2617–30. http://dx.doi.org/10.1109/TSTE.2020.2968507.

[35] del Hoyo Arce I, Herrero López S, López Perez S, Rämä M, Klobut K, Febres JA. Models for fast modelling of district heating and cooling networks. Renew Sustain Energy Rev 2018;82:1863–73. http://dx.doi.org/10.1016/j.rser.2017.06.109.

[36] Jakubek D, Ocłoń P, Nowak-Ocłoń M, Sułowicz M, Varbanov PS, Klemeš JJ. Mathematical modelling and model validation of the heat losses in district heating networks. Energy 2023;267:126460. http://dx.doi.org/10.1016/j.energy.2022.126460.

[37] Lan T, Strunz K. Droop control for district heating networks: Solution for temperature control of multi-energy system with renewable power supply. Int J Electr Power Energy Syst 2023;146:108663. http://dx.doi.org/10.1016/j.ijepes.2022.108663.

[38] Jansen J, Jorissen F, Helsen L. Optimal control of a fourth generation district heating network using an integrated non-linear model predictive controller. Appl Therm Eng 2023;223:120030. http://dx.doi.org/10.1016/j.applthermaleng.2023.120030.

[39] Vandermeulen A, van der Heijde B, Helsen L. Controlling district heating and cooling networks to unlock flexibility: A review. Energy 2018;151:103–15. http://dx.doi.org/10.1016/j.energy.2018.03.034.

[40] Pizzolato A, Sciacovelli A, Verda V. Centralized control of district heating networks during failure events using discrete adjoint sensitivities. Energy 2019;184:58–72. http://dx.doi.org/10.1016/j.energy.2017.09.102, Shaping research in gas-, heat- and electric- energy infrastructures.

[41] Guelpa E, Sciacovelli A, Verda V. Thermo-fluid dynamic model of large district heating networks for the analysis of primary energy savings. Energy 2019;184:34–44. http://dx.doi.org/10.1016/j.energy.2017.07.177, Shaping research in gas-, heat- and electric- energy infrastructures.

[42] Guelpa E, Toro C, Sciacovelli A, Melli R, Sciubba E, Verda V. Optimal operation of large district heating networks through fast fluid-dynamic simulation. Energy 2016;102:586–95. http://dx.doi.org/10.1016/j.energy.2016.02.058.

[43] Sun C, Yuan L, Chen Y, Cao S, Xia G, Qi C, Wu X. An intelligent control and regulation strategy aiming at building level heating balance in district heating system. Energy 2023;278:127941. http://dx.doi.org/10.1016/j.energy.2023.127941.

[44] Bastida H, Ugalde-Loo CE, Abyesekera M, Qadrdan M. Modelling and control of district heating networks with reduced pump utilisation. IET Energy Syst Integr 2021;3(1):13–25. http://dx.doi.org/10.1049/esi2.12001.

[45] Development of multi-level policy plans – action plans for retrofitting of district heating systems. Keep Warm H2020 D5.2, 2020, URL https://keepwarmeurope.eu/fileadmin/user_upload/Resources/Deliverables/KeepWarm_D5.2_Development_of_Multi-level_policy_Plans.pdf.

[46] EU, H2020 ACCEPT Project. 2021, URL https://cordis.europa.eu/project/id/957781.

[47] Shen F, Wu Q, Jin X, Zhou B, Li C, Xu Y. ADMM-based market clearing and optimal flexibility bidding of distribution-level flexibility market for day-ahead congestion management of distribution networks. Int J Electr Power Energy Syst 2020;123:106266. http://dx.doi.org/10.1016/j.ijepes.2020.106266.

[48] Piclo. The leading independent marketplace for flexibility services. 2023, URL https://www.piclo.energy/.

[49] Capriasca Calore. URL http://www.capriascacalore.ch/.

[50] Open Modelica. URL https://openmodelica.org/.

[51] Mermoud F, Haroutunian A, Faessler J, Lachal BM. Impact of load variations on wood boiler efficiency and emissions: in-situ monitoring of two boilers (2 MW and 0.65 MW) supplying a district heating system. Arch Sci 2015;68:27–38, URL https://api.semanticscholar.org/CorpusID:73658184.

[52] Baldi S, Zhang F, Le Quang T, Endel P, Holub O. Passive versus active learning in operation and adaptive maintenance of Heating, Ventilation, and Air Conditioning. Appl Energy 2019;252:113478. http://dx.doi.org/10.1016/j.apenergy.2019.113478.

[53] Vorspel L, Bücker J. District-heating-grid simulation in Python: DiGriPy. Computation 2021;9(6). http://dx.doi.org/10.3390/computation9060072.

[54] Assouline D, Mohajeri N, Gudmundsson A, Scartezzini J-L. A machine learning approach for mapping the very shallow theoretical geothermal potential. Geotherm Energy 2019;7(1):1–50. http://dx.doi.org/10.1186/s40517-019-0135-6.